HHS Public Access

Author manuscript

Brain Stimul. Author manuscript; available in PMC 2023 January 01.

Published in final edited form as:

Brain Stimul. 2022 ; 15(1): 23–31. doi:10.1016/j.brs.2021.11.006.

Deep brain stimulation effect on anterior pallidum reduces motor impulsivity in Parkinson's disease

Khaled Moussawi[1,*,†], **Min Jae Kim**[2,3,†], **Sydney Baybayan**[2], **Myles Wood**[2], **Kelly A. Mills**[2,*]

[1]Department of Psychiatry, School of Medicine, University of Pittsburgh, Pittsburgh, PA, USA

[2]Department of Neurology, School of Medicine, Johns Hopkins University, Baltimore, MD, USA

[3]Department of Biomedical Engineering, School of Medicine, Johns Hopkins University, Baltimore, MD, USA

Abstract

Background—Deep Brain Stimulation (DBS) of the subthalamic nucleus or globus pallidus internus is used to treat the motor symptoms of Parkinson's disease. The former can worsen impulsive and compulsive behaviors after controlling for the reduction of dopaminergic medications. However, the effect of pallidal DBS on such behaviors in PD patients is less clear.

Objective/Hypothesis—We hypothesized that greater stimulation spread to the pallidum with prefrontal connectivity would reduce motor impulsivity.

Methods—Seven Parkinson's patients with stable globus pallidus internus DBS settings for 3 months, disease duration of 13 ±1.3 years, and Montreal Cognitive Assessment of 26.8 ±1.1 each had two stimulation settings defined based on reconstructions of lead placement and volume of tissue activation targeting either a dorsal or ventral position along the DBS electrode but still within the globus pallidus internus. Subjects performed a stop signal reaction time task with the DBS turned off vs. on in each of the defined stimulation settings, which was correlated with the degree of stimulation effect on pallidal subregions.

[*]**Corresponding Author: Kelly A. Mills,** Johns Hopkins University School of Medicine, Dept. of Neurology, Meyer 6-181D, 600 N. Wolfe Street, Baltimore, MD 21287, Phone: 410-502-0133, kmills16@jhmi.edu.

[†]These authors contributed equally to this work

Credit Author Statement:

All authors participated in this research, read the manuscript, and agree with the findings herein. The manuscript is not under consideration by another journal and no ghostwriting by an undisclosed author occurred. The study was performed with approval of the Johns Hopkins Institutional Review Board.

Khaled Moussawi: conceptualization, methodology, formal analysis, writing – review & editing

Min Jae Kim: methodology, formal analysis, data curation, writing – original draft

Sydney Baybayan: investigation

Myles Wood: investigation

Kelly Mills: conceptualization, methodology, formal analysis, investigation, resources, writing – review & editing, supervision, project administration

Author Contributions

Khaled Moussawi: Conceptualization, Methodology, Investigation, Data Curation, Writing – Original Draft, Supervision, Project Administration. **Min Jae Kim**: Methodology, Software, Formal analysis, Writing – Original Draft, Visualization. **Sydney Baybayan**: Investigation, Writing – Review & Editing. **Myles Wood**: Software, Investigation, Writing – Review & Editing. Supervision, Project Administration.

Results—A shorter distance between the volume of tissue activation and the right prefrontally-connected GPi correlated with less impulsivity on the stop signal reaction time task ($r=0.69$, $p<0.05$). Greater volume of tissue activation overlap with the non-prefrontally-connected globus pallidus internus was associated with increased impulsivity.

Conclusion—These data can be leveraged to optimize DBS programming in PD patients with problematic impulsivity or in other disorders involving impulsive behaviors such as substance use disorders.

Keywords

Parkinson's disease; deep brain stimulation; impulsivity; globus pallidus

INTRODUCTION

In addition to the motor symptoms of Parkinson's disease (PD), dopaminergic denervation of the basal ganglia-thalamo-cortical circuitry results in non-motor dysfunctions involving mood, cognition, and behavior [1, 2]. Dopamine replacement, especially the use of dopamine agonists, is associated with the potential development of impulse control disorders (ICD) like hypersexuality and gambling [3]. Treatment of ICD's can be difficult given patients' reliance on dopamine replacement therapy for optimal motor function.

With progression of PD, deep brain stimulation (DBS) of the subthalamic nucleus (STN) or globus pallidus internus (GPi) is considered in some patients to manage worsening motor symptoms. In many patients, DBS also improves medication-related complications like dyskinesia and ICD by reducing the levodopa equivalent daily dose (LEDD) [4]. However, when controlling for the reduction of LEDD, STN DBS was shown to worsen impulsive behaviors across multiple measures [5–9], the degree of which correlates with frontostriatal connectivity [10]. The effects of GPi DBS on impulsivity are less clear, and understanding these effects could have direct clinical implications for programming PD patients with existent GPi DBS and comorbid ICD, especially those whose LEDD requirement is not reduced post-DBS.

Human imaging and primate tracing studies illustrate that the GPi is composed of contiguous subregions that maintain functional and anatomic segregation in "parallel processing loops" throughout the cortico-basal ganglia-thalamo-cortical networks involving various cortical regions [11, 12]. The posterolateral GPi (i.e., sensorimotor GPi) receives inputs from the dorsolateral striatum and is functionally connected to the sensorimotor cortical areas, while the anteromedial GPi (PFC-GPi) receives inputs from the ventral and dorsomedial striatum and is functionally connected to the prefrontal cortical areas. Several reported cases of anterior GPi lesions suggest a role of the anterior GPi in regulating impulsivity and motivation [13, 14]. Further, case series in patients with Tourette's Syndrome, a disorder of motivated movement and its inhibition [15], treated with GPi DBS for refractory tics showed better efficacy when DBS leads were placed in the PFC-GPi, compared to sensorimotor-GPi, the latter being the gold standard target for movement disorders with GPi DBS [16].

Given the differential GPi connectivity profile, the role of the prefrontal cortex in impulsivity [17–19], the DBS results from Tourette's Syndrome studies [16, 20–22], and the potential role of anterior GPi lesions in motivational disorders [13, 14], we hypothesized that GPi DBS reduces impulsivity when the field of stimulation involves the anterior PFC-GPi, and as such, we predicted that in patients with PD implanted with GPi DBS, closer proximity of stimulation to the PFC-GPi correlates with reduced motor impulsivity. As an accepted measure to evaluate prepotent response inhibition across numerous behavioral disorders [23–26], and particularly as a marker for motor impulsivity [27, 28], Stop Signal Reaction Task (SSRT) was adopted to observe the association between motor impulsivity and stimulation effect.

METHODS

Participant Subjects and Screening

Seven patients (5 males, 2 females) meeting Movement Disorders Society Criteria for Clinically Established Parkinson's disease and followed in the Johns Hopkins Neuromodulation and Advanced Therapies Clinic were included in the study. To meet the inclusion criteria, subjects had to be implanted with bilateral GPi DBS, had stable settings for at least 3 months, and were fluent in English. We excluded potential participants who had a history of severe cognitive impairment (MoCA <21) or had a known severe reaction to having DBS turned off for minutes to 2 hours. Subjects were also excluded if either GPi DBS lead position did not allow for two non-overlapping volumes of tissue activation (VTA) of superior (dorsal) and inferior (ventral) stimulation settings.

DBS Stimulation Parameters

Recruited subjects had either directional (Abbott St Jude 6173™) or omnidirectional leads (Medtronic 3387™). Lead location was reconstructed from post-operative CT images co-registered to pre-operative T1 volumetrically acquired MRI images using the MATLAB toolbox Lead DBS [29]. MRI and CT scans were normalized to MNI ICBM 2009b Nonlinear Asymmetric atlas and FEM-based volume of tissue activation (VTA) was created. The position of the reconstructed leads relative to PFC-GPi was determined using a normative atlas [30]. Figure 1A illustrates the lead localizations across participants using a Lead Group toolbox [31]. The active clinically programmed contact location, polarity, and settings varied across subjects. The DBS pulse-width ranged between 60 and 90 msec, frequency 130 to 150 Hz, and stimulation intensity 2 to 5 mV / mA.

Subjects underwent behavioral testing with three experimental conditions (Figure 1B, E): 1) DBS-ON-ventral condition where the most inferior contact within the GPi was activated (Figure 1B-left), 2) DBS-ON-dorsal where the most superior contact within the GPi was activated (Figure 1B-right), and 3) DBS-OFF. The order of different DBS conditions was pseudorandomized. The ventral and dorsal stimulation settings were chosen to maximize spatial distinction between ventral and dorsal VTAs which were used in the correlations with the behavioral measures [30]. Overlap between ventral and dorsal VTA was avoided. Due to the typical trajectory of GPi DBS electrodes, the dorsal VTA was typically more anterior than the ventral VTA. During the testing sessions, patients were slowly ramped up

to the goal amplitude as determined by the VTA modeling, with a consistent frequency of 130 Hz and pulse width of 60 μsec across all participants in all experimental conditions. The amplitude ramp was stopped just below the threshold of any reported side effects from stimulation.

Experimental paradigm

Participants underwent testing with three experimental conditions (DBS-OFF, DBS-ON-ventral, and DBS-ON-dorsal) across two separate visits, 1–2 weeks apart, and two sessions per visit (Figure 1E). Each visit was scheduled for 5 hours and included one DBS-OFF session and one DBS-ON (ventral or dorsal) session (2.5 hours per session). The DBS-OFF session was repeated between visits to control for variation in baseline behavioral function across testing days. The order of DBS-ON-ventral vs. DBS-ON-dorsal across visits was chosen at random.

The subjects arrived at 08:00 after withholding their dopamine replacement medications overnight and took their Levodopa and dopamine agonist medications at the prescribed dose under direct observation. Subjects were tested in the medication “on” state to control for the effect of dopamine replacement and isolate the effect of stimulation and to avoid distraction from the task by intolerable motor symptoms in the med-OFF, DBS-OFF state. A clinician activated the DBS settings determined by VTA modeling for each testing session with the testing research assistant out of the room and if there were immediate side effects, reduced the voltage or amplitude to below the side effect threshold. The unblinded clinician left the testing room for the entire testing session but remained nearby in case intolerable side effects occurred. A 30 min wash-in or wash-out period followed DBS adjustments (Figure 1E). Patients did not eat during the sessions but were allowed to drink water and to take their medications as prescribed to avoid a wearing-off effect. The subjects and testing research assistant were blinded to the stimulation condition.

Stop Signal Reaction Time Task

Stimuli were presented on a computer monitor using e-Prime software (version 2.0, Psychology Software Tools, Sharpsburg, PA). Each trial began with a black fixation cross centered on a white background. After 500 msec, a black square (Go Signal) appeared equiprobably to either the right or the left side of the cross. Subjects responded accordingly by pressing either the left or right arrow key with the right hand, regardless of handedness or motor symptom asymmetry, corresponding to the side the square appeared. On 25% of the trials, the black square turned red (stop signal) after a variable delay (stop signal delay, SSD). SSD was varied using a dynamic tracking staircase procedure [24, 32]. The SSD value was selected from one of four staircases which started with SSD values of 100,150, 200, and 250 msec. If the subject failed to stop after a stop signal, the delay was made 50 msec smaller making it easier to inhibit the response on the following stop signal trial. If the subject stopped successfully, the delay was made 50 msec longer on the following stop signal trial. The subjects underwent testing in 3 blocks per session, where each block consisted of 32 stop trials and 96 go trials (total 128 trials/block). Each staircase moved 8 times within each block (4 staircases for 32 stop trials). The staircases were independent but randomly interleaved, meaning that each particular stop trial pertained to

one particular staircase, but the order of staircases was randomized on a trial-by-trial basis. This arrangement allowed a stopping probability close to 50% by the end of the experiment.

Analysis of Stop Signal Reaction Time

The Stop Signal Reaction Time (SSRT) for each session was calculated using the convergence method [17, 32]. SSRT was calculated for one block and averaged between the three blocks/session. For each block, SSRT was calculated as mean Go reaction time (average of reaction time on all correct go trials in the block) minus mean SSD of all 4 staircases after convergence (each staircase SSD was the mean of the last 3 or 4 SSD values in that staircase, when stopping probability was close to 50%). SSRT for each session was the average SSRT of the 3 blocks. The SSRT served as a marker of inhibitory control such that higher SSRT corresponded to reduced efficiency of inhibiting a prepotent motor response, one component of the multifactorial construct of impulsivity.

Distance Metrics between VTA and PFC-GPi

The reconstruction of lead locations revealed that all leads were placed in the posterior sensorimotor-GPi (Figure 1A), and VTA simulations showed little to no-overlap of VTAs with the PFC-GPi, which prevented volumetric overlap assessment of VTA with PFC-GPi across the entire group. However, the anterior position of the PFC-GPi relative to sensorimotor-GPi and the antero-posterior angle of lead implantation provided a spatial distribution of the VTAs (dorsal and ventral) relative to PFC-GPi. Acknowledging that the volume boundaries of VTA correspond to a specific electric field threshold (0.2 V/mm) [33, 34], and that the activation threshold of axons is highly variable based on tissue properties [35] such that neural tissue beyond the defined VTA is still impacted by smaller electric fields, we measured the distance between each VTA and the PFC-GPi centroid with the assumption that shorter *vs.* longer distances between the VTA and PFC-GPi correlate with stronger *vs.* weaker effects of DBS on the PFC-GPi subregion (Figure 1C). The centroid coordinate of the PFC-GPi was evaluated as the arithmetic mean of all spatial coordinates comprising its volume. The distance was measured as the minimum Euclidean distance formed between the centroid coordinate of the PFC-GPi among the coordinates comprising the surface of the VTA (Figure 1C).

Volumetric overlap between VTA and GPi

The volumetric overlap between the VTA and overall GPi was calculated using a built-in function in the Lead DBS toolbox, which calculates the individual volumes of surface triangulation of VTA and GPi, and subsequently extracts the volume of the intersecting region (Figure 1D). While the VTA estimation was not validated by another method, prior studies in Parkinson's disease [36, 37], essential tremor [38], and dystonia [39] have shown a good correlation between VTA overlap with target structure and clinical outcomes.

Data Analysis

One-way ANOVA was used to assess for differences in variance of GO-RT, SSRT, and SSD between the three stimulation conditions (OFF, ON-ventral, and ON-dorsal) regardless of VTA location. Because Go-RT and SSRT values are measured twice in the DBS OFF

condition, once at each study visit, the average values of the two OFF-condition Go-RT and SSRT values were reported. The correlation between GO-RT or SSRT and the distance between the VTA and PFC-GPi or volume overlap between VTA and GPi was evaluated with Spearman's Rho coefficient using GraphPad Prism (version 9.1.0). Outliers were identified using Grubb's test with α=0.05. One data point in the volume overlap analysis was excluded as an extreme outlier. Statistical significance was set at p<0.05. Data are presented as mean ± S.E.M.

RESULTS

Demographics of study participants

The average age of the participants was 62.6 years, with a mean disease duration of 13 years, mean duration of DBS implantation of 12.1 months, and mean UPDRS Part III score 32.6 (on medications with clinically optimized DBS-ON) (Table 1). The stimulation settings used for DBS-ventral and DBS-dorsal conditions for each participant are reported in Table 3. The Montreal Cognitive Assessment (MoCA) was performed during clinically optimized DBS settings. The subjects had minimal to no cognitive impairment during their participation in the study.

Go-Reaction Time

There was no overall difference in the Go-Reaction Time (GO-RT), a measure of proactive response initiation, between the DBS-OFF *vs.* DBS-ON conditions (Table 2). However, the distance between right PFC-GPi centroid and VTA was significantly correlated with the change in GO-RT between DBS-ON and OFF conditions (r = 0.77, $p < 0.005$, Figure 2A). These results indicate that a shorter distance between VTA and PFC-GPi, which likely causes stronger electric fields in the PFC-GPi, correlates with faster GO-RT during the SSRT task. This correlation was specific to the right hemisphere as there was no correlation between left PFC-GPi centroid and VTA (r = 0.06, $p = 0.83$) (Figure 2A).

To examine the DBS effect of non-PFC GPi on GO-RT, we evaluated the correlation between volumetric overlap of VTA and overall GPi (since there was minimal to no overlap of VTA with PFC-GPi). The volumetric overlap of VTA and left GPi was positively correlated with GO-RT (r = 0.58, p < 0.05, Figure 2B). No significant correlation was observed with the right GPi (r = 0.46, $p = 0.12$, Figure 2B). These results suggest that DBS of a larger volume of the sensorimotor GPi is correlated with slower motor initiation. Of note, there was no correlation of response accuracy (successfully stopping when a stop cue was presented) with the distance between VTA and PFC-GPi or volumetric overlap of VTA with GPi in either hemisphere.

Stop-Signal Reaction Time

SSRT represents the degree of reactive inhibition following a cue. A longer SSRT indicates that a stop signal must be presented closer to the Go signal to allow the subject to successfully inhibit their response and suggests increased impulsivity (worse motor inhibition). On the other hand, a shorter SSRT indicates the subject is able to inhibit their response even when the stop signal is presented late and suggests reduced impulsivity.

Overall, there was no difference in SSRT between the three DBS conditions when the VTA location was not accounted for (Table 2). Given the role of prefrontal-striatal circuits in impulsivity, [14] we tested the effects of the distance between PFC-GPi and VTA on SSRT. The right PFC-GPi distance from the VTA surface was positively correlated with the change in SSRT between the DBS-ON and OFF settings (r = 0.69, p <0.05, Figure 3A). There was no such correlation in the left hemisphere (r = 0.09, p = 0.75, Figure 3A). These results suggest that motor impulsivity is greater the more distant the VTA is from the PFC-GPi and lower the closer the VTA is to the PFC-GPi. Regression analysis reveals an X intercept of ~4.5mm with negative SSRT difference before that and positive difference after. These results indicate that when the VTA surface is less than the 4.5 mm from the PFC-GPi centroid, DBS will likely result in reduced impulsivity. On the other hand, at distances >4.5 mm, DBS results in increased impulsivity.

To test the specificity of these findings relating right PFC-GPi DBS to impulsivity, we tested the relationship of non-PFC-GPi DBS with SSRT performance. Given the large overlap of VTA with non-PFC GPi, we measured the volumetric overlap of VTA and non-PFC GPi (instead of distance metrics), and correlated it to the difference in SSRT between DBS-ON and OFF. We observed a positive correlation for left GPi with SSRT (left: r = 0.73, p < 0.05, Figure 3B) and a strong trend for the same association between right GPi and SSRT (r = 0.53, p = 0.06), suggesting that greater overlap between VTA and non-PFC GPi results in increased impulsivity. These results support the specificity of the potential role of PFC GPi stimulation in reducing impulsivity.

DISCUSSION

We have shown that while holding dopamine replacement therapy constant, GPi stimulation closer to the GPi subregion with prefrontal connectivity correlates with shorter SSRT, indicating an improvement in motor impulsivity. This correlation between SSRT and the degree of stimulation effect was specific to the PFC-GPi in that a larger volume of tissue activation in the posterior GPi (i.e., the non-PFC-GPi) reversed this association. We believe these results will have important implications for future studies of the effects of lead location on non-motor DBS outcomes in PD patients and could be translated to other disorders involving motor impulse control such as Tourette’s syndrome and substance use disorders.

Worsening impulsivity and inducing Impulse Control Disorders (ICDs) are two major complications of dopamine replacement therapy in PD patients. After STN DBS implantation, dopamine replacement is usually reduced. However, the interplay between the intrinsic disease impact and the effects of DBS and ensuing medication reduction on impulsivity is complex. While many patients with STN DBS show nearly 50% reduction of LEDD following STN DBS [40], with an associated improvement of dyskinesia [41–43] and ICD [4, 44–47], other patients continue to require high doses of dopaminergic medications as reflected in their unchanged LEDD [48]. The ICD prevalence does not improve in patients who do not show reduced LEDD post-DBS [4]. Importantly, STN DBS was shown to worsen impulsive behaviors across multiple measures after controlling for the reduction of dopamine replacement dosage [5–9]. As such, in patients whose LEDD remains unchanged post-DBS, STN DBS increases hyperdopaminergic behaviors like ICD

and Dopamine Dysregulation Syndrome (DDS), which is reminiscent of the exacerbation of dyskinesia in those patients. Alternatively, some DBS centers target the GPi due to better cognitive side effects profile and improved mood outcomes compared to STN DBS [48–50]. GPi DBS directly mitigates dyskinesia in PD patients without requiring LEDD reduction [51]. Therefore, GPi DBS may be used in patients with significant dyskinesias who cannot tolerate LEDD reduction lest this causes worsening apathy and axial symptoms [52]. Our finding of reduced impulsivity being association with VTA's that are closer in proximity to the PFC-GPi vis-à-vis the previously reported increased impulsivity with STN DBS mirrors the contrasting effects of sensorimotor GPi *vs.* STN stimulation on dyskinesia, when LEDD is unchanged [4, 10].

Our results show that effects of GPi DBS on impulsivity are more nuanced than STN DBS and vary with the VTA in relation to the PFC-GPi subregion. The correlation between stimulation effect on motor impulsivity and the proximity of stimulation to PFC-GPi was localized to the right hemisphere, which is consistent with prior literature on the neurocircuitry of motor impulsivity [53]. Reactive inhibition, as in the SSRT task, has been repeatedly shown to depend on the right dorsolateral PFC, including the precentral gyrus, pre-supplementary motor area, and inferior frontal gyrus [18, 19, 54, 55].

While increased stimulation of PFC-GPi was associated with reduced impulsivity, it was also associated with faster motor initiation as indicated by reduced Go-RT. This latter effect is consistent with prior literature showing that DBS stimulation of PFC connected circuits reduces reaction time [56]. This is likely due to improved attention processes and cognitive control during tasks that emphasize speed of motor initiation [56–61].

To determine whether this correlation is specific to stimulation of the PFC-GPi *vs.* other pallidal subregions, we showed that increased VTA overlap with non-PFC GPi was associated with the opposite outcome (i.e., greater overlap is correlated with increased impulsivity). One explanation is that a larger overlap between VTA and non-PFC-GPi translates to reduced stimulation effect on the PFC-GPi, and therefore increased impulsivity. Alternatively, it is possible that DBS of the premotor-GPi causes functional inhibition of the pallidal GABAergic neurons, which results in disinhibition of the downstream thalamocortical circuits and increased activation of the premotor cortex, thus increasing the tendency of the motor cortex to generate a response. Lastly, the effect of a larger VTA overlap non-PFC-GPi could be confounded by extent of VTA overlap with GPe, the effects of which on impulsive behaviors remain largely unexplored.

While trying to leverage the unique opportunity DBS offers in causing reversible lesion-like effects to explore behavioral-anatomic relationships, this approach has some limitations. For example, the experimental paradigm involved simultaneous bilateral stimulation in either ventral or dorsal positions within the GPi. We did not test the stimulation effect of each hemisphere independently. To optimize the experimental design and capture behavioral responses in the same medication state ("on" medications), we asked participants to arrive to the office on testing days in the "off" state. Testing each hemisphere independently would have required two more testing visits, which adds significant burden to participants. Another limitation of this study is the correlational nature of the results as opposed to demonstrating

a causal relationship between PFC-GPi stimulation and reduced impulsivity. The DBS electrodes in all the participants were localized to the sensorimotor GPi, and therefore, establishing a causal relationship cannot be attained considering the opposite correlational patterns we observed between stimulating PFC- *vs.* non-PFC GPi. However, case studies of anterior GPi lesions suggest a causal role of PFC-GPi in regulating impulsive behaviors [13, 14]. Further, data from Tourette's syndrome patients implanted with PFC-GPi DBS provide supportive evidence regarding PFC-GPi DBS effects on reducing impulsivity – PFC-GPi DBS in the treatment of refractory Tourette's, which is strongly associated with impulsivity [62], has been shown to be more efficacious than sensorimotor-GPi DBS [20–22].

While the number of patients enrolled in this study was small, each patient contributed two data points (ventral vs. dorsal electrode contact). That the study detected a correlation between stimulation intensity and behavioral outcome in a small cohort speaks to the strength of this structure-function association. The rigor of the data analysis and conclusion was reflected in the specificity of main finding to the right hemisphere, which is consistent with the SSRT literature [18, 19, 53–55]. Overall, the main hypothesis of this study, that stimulation of PFC-GPi reduces impulsivity compared to sensorimotor-GPi DBS, is ideally best tested in a study design where both GPi areas are directly implanted with DBS leads, which allows for direct comparison. While our findings may motivate this approach in future research, our goal was to leverage the placement of GPi leads targeting motor parkinsonism to explore effects on a non-motor GPi region of interest and potentially generate data to support this approach.

The primary motivation behind our study was to understand the distinctive effects of DBS of the different GPi subregions on regulating impulsivity. Our findings support the hypothesis that right PFC-GPi DBS reduces impulsivity. Future clinical studies could be performed to test whether comorbid ICD mitigation is possible without a substantial LEDD reduction following PFC-GPi DBS and whether this region could be targeted for other disorders involving impulsive behaviors.

Funding:

Kelly Mills' effort was supported by NIH/NINDS 5K23NS101096-04.

Declaration of interest

Kelly Mills received grant funding from the NIH/NINDS, the Michael J. Fox Foundation, the Parkinson Foundation and research support from Global Kinetics Corporation. Khaled Moussawi received funding as salary support from the NIH/NIDA and NIH/NIDA research support under grant DA048085-02. Sydney Baybayan received funding from the Michael J. Fox Foundation and Parkinson's Foundation as salary support for research.

Myles Wood reports no funding or disclosures. Min Jae Kim reports no funding or disclosures.

REFERENCES

[1]. Chaudhuri KR, Schapira AH. Non-motor symptoms of Parkinson's disease: dopaminergic pathophysiology and treatment. Lancet Neurol 2009;8(5):464–74. [PubMed: 19375664]

[2]. Remy P, Doder M, Lees A, Turjanski N, Brooks D. Depression in Parkinson's disease: loss of dopamine and noradrenaline innervation in the limbic system. Brain 2005;128(Pt 6):1314–22. [PubMed: 15716302]

[3]. Weintraub D. Dopamine and impulse control disorders in Parkinson's disease. Ann Neurol 2008;64 Suppl 2(Suppl 2):S93–100. [PubMed: 19127573]

[4]. Santin MDN, Voulleminot P, Vrillon A, Hainque E, Béreau M, Lagha-Boukbiza O, et al. Impact of Subthalamic Deep Brain Stimulation on Impulse Control Disorders in Parkinson's Disease: A Prospective Study. Mov Disord 2021;36(3):750–7. [PubMed: 33022101]

[5]. Ballanger B, van Eimeren T, Moro E, Lozano AM, Hamani C, Boulinguez P, et al. Stimulation of the subthalamic nucleus and impulsivity: release your horses. Ann Neurol 2009;66(6):817–24. [PubMed: 20035509]

[6]. Hagelweide K, Schönberger AR, Kracht LW, Gründler TOJ, Fink GR, Schubotz RI. Motor cognition in patients treated with subthalamic nucleus deep brain stimulation: Limits of compensatory overactivity in Parkinson's disease. Neuropsychologia 2018;117:491–9. [PubMed: 30003903]

[7]. Hälbig TD, Tse W, Frisina PG, Baker BR, Hollander E, Shapiro H, et al. Subthalamic deep brain stimulation and impulse control in Parkinson's disease. Eur J Neurol 2009;16(4):493–7. [PubMed: 19236471]

[8]. Evens R, Stankevich Y, Dshemuchadse M, Storch A, Wolz M, Reichmann H, et al. The impact of Parkinson's disease and subthalamic deep brain stimulation on reward processing. Neuropsychologia 2015;75:11–9. [PubMed: 25976111]

[9]. Frank MJ. Hold your horses: a dynamic computational role for the subthalamic nucleus in decision making. Neural Netw 2006;19(8):1120–36. [PubMed: 16945502]

[10]. Mosley PE, Paliwal S, Robinson K, Coyne T, Silburn P, Tittgemeyer M, et al. The structural connectivity of subthalamic deep brain stimulation correlates with impulsivity in Parkinson's disease. Brain 2020;143(7):2235–54. [PubMed: 32568370]

[11]. Bertino S, Basile GA, Bramanti A, Anastasi GP, Quartarone A, Milardi D, et al. Spatially coherent and topographically organized pathways of the human globus pallidus. Hum Brain Mapp 2020;41(16):4641–61. [PubMed: 32757349]

[12]. Draganski B, Kherif F, Klöppel S, Cook PA, Alexander DC, Parker GJ, et al. Evidence for segregated and integrative connectivity patterns in the human Basal Ganglia. J Neurosci 2008;28(28):7143–52. [PubMed: 18614684]

[13]. Moussawi K, Kalivas PW, Lee JW. Abstinence From Drug Dependence After Bilateral Globus Pallidus Hypoxic-Ischemic Injury. Biol Psychiatry 2016;80(9):e79–e80. [PubMed: 27311800]

[14]. Miller JM, Vorel SR, Tranguch AJ, Kenny ET, Mazzoni P, van Gorp WG, et al. Anhedonia after a selective bilateral lesion of the globus pallidus. Am J Psychiatry 2006;163(5):786–8. [PubMed: 16648316]

[15]. Frank MC, Piedad J, Rickards H, Cavanna AE. The role of impulse control disorders in Tourette syndrome: an exploratory study. J Neurol Sci 2011;310(1–2):276–8. [PubMed: 21741055]

[16]. Martínez-Fernández R, Zrinzo L, Aviles-Olmos I, Hariz M, Martinez-Torres I, Joyce E, et al. Deep brain stimulation for Gilles de la Tourette syndrome: a case series targeting subregions of the globus pallidus internus. Mov Disord 2011;26(10):1922–30. [PubMed: 21538528]

[17]. Aron AR, Fletcher PC, Bullmore ET, Sahakian BJ, Robbins TW. Stop-signal inhibition disrupted by damage to right inferior frontal gyrus in humans. Nat Neurosci 2003;6(2):115–6. [PubMed: 12536210]

[18]. Aron AR, Robbins TW, Poldrack RA. Inhibition and the right inferior frontal cortex. Trends Cogn Sci 2004;8(4):170–7. [PubMed: 15050513]

[19]. Smith JL, Jamadar S, Provost AL, Michie PT. Motor and non-motor inhibition in the Go/NoGo task: an ERP and fMRI study. Int J Psychophysiol 2013;87(3):244–53. [PubMed: 22885679]

[20]. Servello D, Galbiati TF, Balestrino R, Iess G, Zekaj E, Michele S, et al. Deep Brain Stimulation for Gilles de la Tourette Syndrome: Toward Limbic Targets. Brain Sci 2020;10(5).

[21]. Martinez-Ramirez D, Jimenez-Shahed J, Leckman JF, Porta M, Servello D, Meng FG, et al. Efficacy and Safety of Deep Brain Stimulation in Tourette Syndrome: The International Tourette Syndrome Deep Brain Stimulation Public Database and Registry. JAMA Neurol 2018;75(3):353–9. [PubMed: 29340590]

[22]. Johnson KA, Duffley G, Foltynie T, Hariz M, Zrinzo L, Joyce EM, et al. Basal Ganglia Pathways Associated With Therapeutic Pallidal Deep Brain Stimulation for Tourette Syndrome. Biol Psychiatry Cogn Neurosci Neuroimaging 2020.

[23]. Verbruggen F, Aron AR, Band GPH, Beste C, Bissett PG, Brockett AT, et al. A consensus guide to capturing the ability to inhibit actions and impulsive behaviors in the stop-signal task. eLife 2019;8:e46323. [PubMed: 31033438]

[24]. Eagle DM, Baunez C, Hutcheson DM, Lehmann O, Shah AP, Robbins TW. Stop-signal reaction-time task performance: role of prefrontal cortex and subthalamic nucleus. Cereb Cortex 2008;18(1):178–88. [PubMed: 17517682]

[25]. Bartholdy S, Dalton B, O'Daly OG, Campbell IC, Schmidt U. A systematic review of the relationship between eating, weight and inhibitory control using the stop signal task. Neurosci Biobehav Rev 2016;64:35–62. [PubMed: 26900651]

[26]. Lipszyc J, Schachar R. Inhibitory control and psychopathology: a meta-analysis of studies using the stop signal task. J Int Neuropsychol Soc 2010;16(6):1064–76. [PubMed: 20719043]

[27]. Chowdhury NS, Livesey EJ, Blaszczynski A, Harris JA. Pathological Gambling and Motor Impulsivity: A Systematic Review with Meta-Analysis. J Gambl Stud 2017;33(4):1213–39. [PubMed: 28255940]

[28]. Logan GD, Schachar RJ, Tannock R. Impulsivity and Inhibitory Control. Psychological Science 1997;8(1):60–4.

[29]. Horn A, Kühn AA. Lead-DBS: a toolbox for deep brain stimulation electrode localizations and visualizations. Neuroimage 2015;107:127–35. [PubMed: 25498389]

[30]. Ewert S, Plettig P, Li N, Chakravarty MM, Collins DL, Herrington TM, et al. Toward defining deep brain stimulation targets in MNI space: A subcortical atlas based on multimodal MRI, histology and structural connectivity. Neuroimage 2018;170:271–82. [PubMed: 28536045]

[31]. Treu S, Strange B, Oxenford S, Neumann WJ, Kühn A, Li N, et al. Deep brain stimulation: Imaging on a group level. Neuroimage 2020;219:117018. [PubMed: 32505698]

[32]. Swann N, Poizner H, Houser M, Gould S, Greenhouse I, Cai W, et al. Deep brain stimulation of the subthalamic nucleus alters the cortical profile of response inhibition in the beta frequency band: a scalp EEG study in Parkinson's disease. J Neurosci 2011;31(15):5721–9. [PubMed: 21490213]

[33]. Aström M, Tripoliti E, Hariz MI, Zrinzo LU, Martinez-Torres I, Limousin P, et al. Patient-specific model-based investigation of speech intelligibility and movement during deep brain stimulation. Stereotact Funct Neurosurg 2010;88(4):224–33. [PubMed: 20460952]

[34]. Vasques X, Cif L, Hess O, Gavarini S, Mennessier G, Coubes P. Stereotactic model of the electrical distribution within the internal globus pallidus during deep brain stimulation. Journal of Computational Neuroscience 2008;26(1):109. [PubMed: 18553218]

[35]. Astrom M, Diczfalusy E, Martens H, Wardell K. Relationship between neural activation and electric field distribution during deep brain stimulation. IEEE Trans Biomed Eng 2015;62(2):664–72. [PubMed: 25350910]

[36]. Boutet A, Germann J, Gwun D, Loh A, Elias GJB, Neudorfer C, et al. Sign-specific stimulation 'hot' and 'cold' spots in Parkinson's disease validated with machine learning. Brain Commun 2021;3(2):fcab027. [PubMed: 33870190]

[37]. Zhang F, Wang F, Li W, Wang N, Han C, Fan S, et al. Relationship between electrode position of deep brain stimulation and motor symptoms of Parkinson's disease. BMC Neurol 2021;21(1):122. [PubMed: 33731033]

[38]. Al-Fatly B, Ewert S, Kübler D, Kroneberg D, Horn A, Kühn AA. Connectivity profile of thalamic deep brain stimulation to effectively treat essential tremor. Brain 2019;142(10):3086–98. [PubMed: 31377766]

[39]. Coblentz A, Elias GJB, Boutet A, Germann J, Algarni M, Oliveira LM, et al. Mapping efficacious deep brain stimulation for pediatric dystonia. J Neurosurg Pediatr 2021:1–11.

[40]. Alexoudi A, Shalash A, Knudsen K, Witt K, Mehdorn M, Volkmann J, et al. The medical treatment of patients with Parkinson's disease receiving subthalamic neurostimulation. Parkinsonism Relat Disord 2015;21(6):555–60; discussion [PubMed: 25842260]

[41]. Vingerhoets FJ, Villemure JG, Temperli P, Pollo C, Pralong E, Ghika J. Subthalamic DBS replaces levodopa in Parkinson's disease: two-year follow-up. Neurology 2002;58(3):396–401. [PubMed: 11839838]

[42]. Russmann H, Ghika J, Combrement P, Villemure JG, Bogousslavsky J, Burkhard PR, et al. L-dopa-induced dyskinesia improvement after STN-DBS depends upon medication reduction. Neurology 2004;63(1):153–5. [PubMed: 15249627]

[43]. Kleiner-Fisman G, Herzog J, Fisman DN, Tamma F, Lyons KE, Pahwa R, et al. Subthalamic nucleus deep brain stimulation: summary and meta-analysis of outcomes. Mov Disord 2006;21 Suppl 14:S290–304. [PubMed: 16892449]

[44]. Averbeck BB, O'Sullivan SS, Djamshidian A. Impulsive and compulsive behaviors in Parkinson's disease. Annu Rev Clin Psychol 2014;10:553–80. [PubMed: 24313567]

[45]. Merola A, Romagnolo A, Rizzi L, Rizzone MG, Zibetti M, Lanotte M, et al. Impulse control behaviors and subthalamic deep brain stimulation in Parkinson disease. J Neurol 2017;264(1):40–8. [PubMed: 27761641]

[46]. Amami P, Dekker I, Piacentini S, Ferré F, Romito LM, Franzini A, et al. Impulse control behaviours in patients with Parkinson's disease after subthalamic deep brain stimulation: de novo cases and 3-year follow-up. J Neurol Neurosurg Psychiatry 2015;86(5):562–4. [PubMed: 25012201]

[47]. Castrioto A, Funkiewiez A, Debû B, Cools R, Lhommée E, Ardouin C, et al. Iowa gambling task impairment in Parkinson's disease can be normalised by reduction of dopaminergic medication after subthalamic stimulation. J Neurol Neurosurg Psychiatry 2015;86(2):186–90. [PubMed: 24860137]

[48]. Follett KA, Weaver FM, Stern M, Hur K, Harris CL, Luo P, et al. Pallidal versus subthalamic deep-brain stimulation for Parkinson's disease. N Engl J Med 2010;362(22):2077–91. [PubMed: 20519680]

[49]. Okun MS, Wu SS, Fayad S, Ward H, Bowers D, Rosado C, et al. Acute and Chronic Mood and Apathy Outcomes from a randomized study of unilateral STN and GPi DBS. PLoS One 2014;9(12):e114140. [PubMed: 25469706]

[50]. Zahodne LB, Okun MS, Foote KD, Fernandez HH, Rodriguez RL, Wu SS, et al. Greater improvement in quality of life following unilateral deep brain stimulation surgery in the globus pallidus as compared to the subthalamic nucleus. J Neurol 2009;256(8):1321–9. [PubMed: 19363633]

[51]. Moro E, Lozano AM, Pollak P, Agid Y, Rehncrona S, Volkmann J, et al. Long-term results of a multicenter study on subthalamic and pallidal stimulation in Parkinson's disease. Mov Disord 2010;25(5):578–86. [PubMed: 20213817]

[52]. Czernecki V, Schüpbach M, Yaici S, Lévy R, Bardinet E, Yelnik J, et al. Apathy following subthalamic stimulation in Parkinson disease: a dopamine responsive symptom. Mov Disord 2008;23(7):964–9. [PubMed: 18398913]

[53]. Dalley JW, Robbins TW. Fractionating impulsivity: neuropsychiatric implications. Nat Rev Neurosci 2017;18(3):158–71.

[54]. Aron AR, Poldrack RA. Cortical and subcortical contributions to Stop signal response inhibition: role of the subthalamic nucleus. J Neurosci 2006;26(9):2424–33. [PubMed: 16510720]

[55]. Garavan H, Hester R, Murphy K, Fassbender C, Kelly C. Individual differences in the functional neuroanatomy of inhibitory control. Brain Res 2006;1105(1):130–42. [PubMed: 16650836]

[56]. Widge AS, Zorowitz S, Basu I, Paulk AC, Cash SS, Eskandar EN, et al. Deep brain stimulation of the internal capsule enhances human cognitive control and prefrontal cortex function. Nat Commun 2019;10(1):1536. [PubMed: 30948727]

[57]. van Veen V, Krug MK, Carter CS. The neural and computational basis of controlled speed-accuracy tradeoff during task performance. J Cogn Neurosci 2008;20(11):1952–65. [PubMed: 18416686]

[58]. Perri RL, Berchicci M, Spinelli D, Di Russo F. Individual differences in response speed and accuracy are associated to specific brain activities of two interacting systems. Front Behav Neurosci 2014;8:251. [PubMed: 25100961]

[59]. Forstmann BU, van den Wildenberg WP, Ridderinkhof KR. Neural mechanisms, temporal dynamics, and individual differences in interference control. J Cogn Neurosci 2008;20(10):1854–65. [PubMed: 18370596]

[60]. Milham MP, Banich MT, Webb A, Barad V, Cohen NJ, Wszalek T, et al. The relative involvement of anterior cingulate and prefrontal cortex in attentional control depends on nature of conflict. Brain Res Cogn Brain Res 2001;12(3):467–73. [PubMed: 11689307]

[61]. Forstmann BU, Dutilh G, Brown S, Neumann J, von Cramon DY, Ridderinkhof KR, et al. Striatum and pre-SMA facilitate decision-making under time pressure. Proc Natl Acad Sci U S A 2008;105(45):17538–42. [PubMed: 18981414]

[62]. Atkinson-Clement C, Porte CA, de Liege A, Klein Y, Delorme C, Beranger B, et al. Impulsive prepotent actions and tics in Tourette disorder underpinned by a common neural network. Mol Psychiatry 2020.

Highlights:

- Exact location of stimulation within the GPi can modulate motor impulsivity
- GPi stimulation closer to right anterior GPi reduced motor impulsivity
- Larger overlap of stimulation field with left posterior GPi worsened motor impulsivity

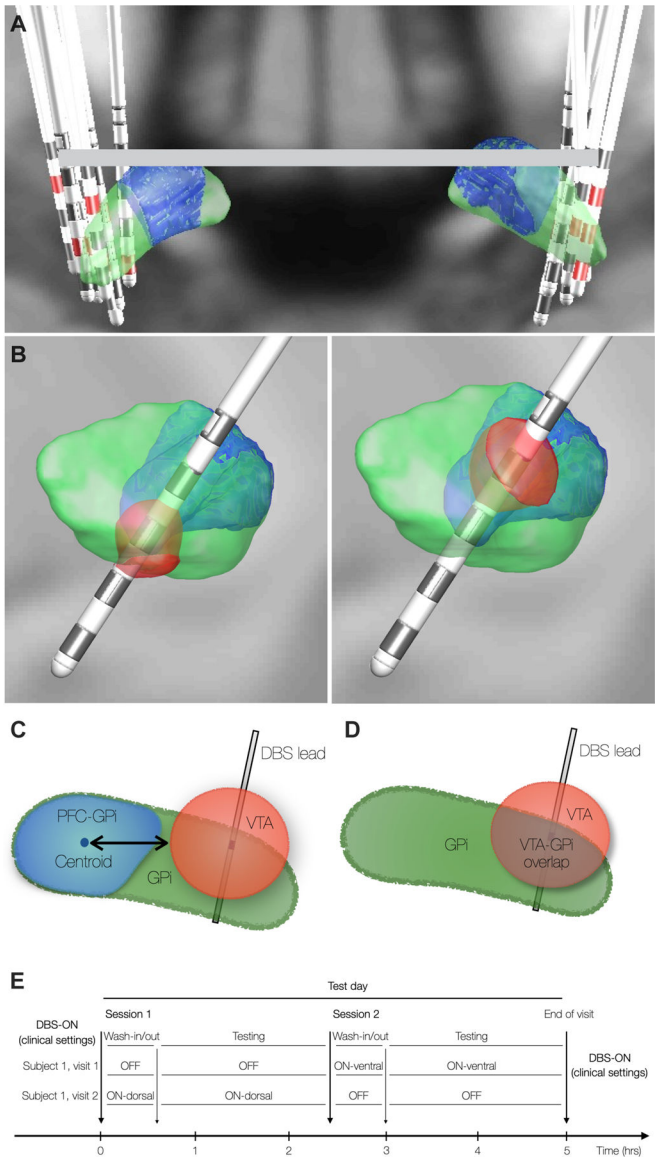

Figure 1. DBS Stimulation Parameters and Experimental Paradigm

(A) DBS lead localization in all subjects. Green = GPi. Blue = GPi subregion with prefrontal cortex connectivity; PFC-GPi). Red = active clinical contact. (B) Simulated Volumes of Tissue Activation (VTA) in the “ventral” (left) and “dorsal” (right) conditions. Impact of stimulation measured with either distance of VTA surface to PFC-GPi centroid (C) or VTA overlap with target (D). (E) Experimental design with 3 DBS conditions: OFF, ON-dorsal, ON-ventral.

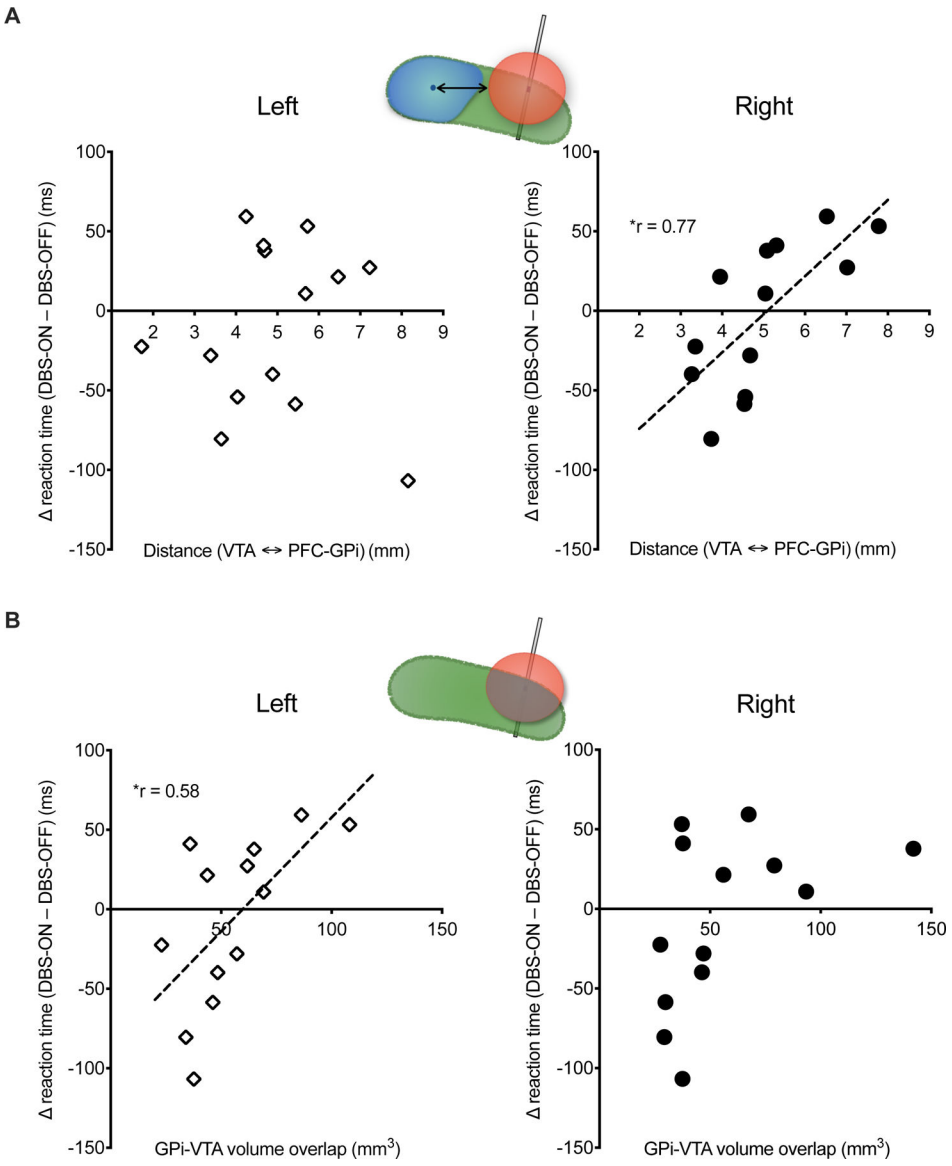

Figure 2. Go-Reaction Time and PFC-GPi Stimulation

Correlation between Go-Reaction Time (GO-RT) and DBS volume of tissue activation (VTA). (A) Shorter distance between the right PFC-GPi centroid and VTA is correlated with shorter GO-RT during the SSRT task. (B) Greater volumetric overlap between VTA and left GPi correlates with longer GO-RT during the SSRT task. Cartoons in each panel illustrate the metrics used in the correlation analysis (see Figure 1 C, D for details). Left and Right indicate left *vs.* right hemisphere DBS. r = Spearman's correlation coefficient. * indicates significance (p <0.05).

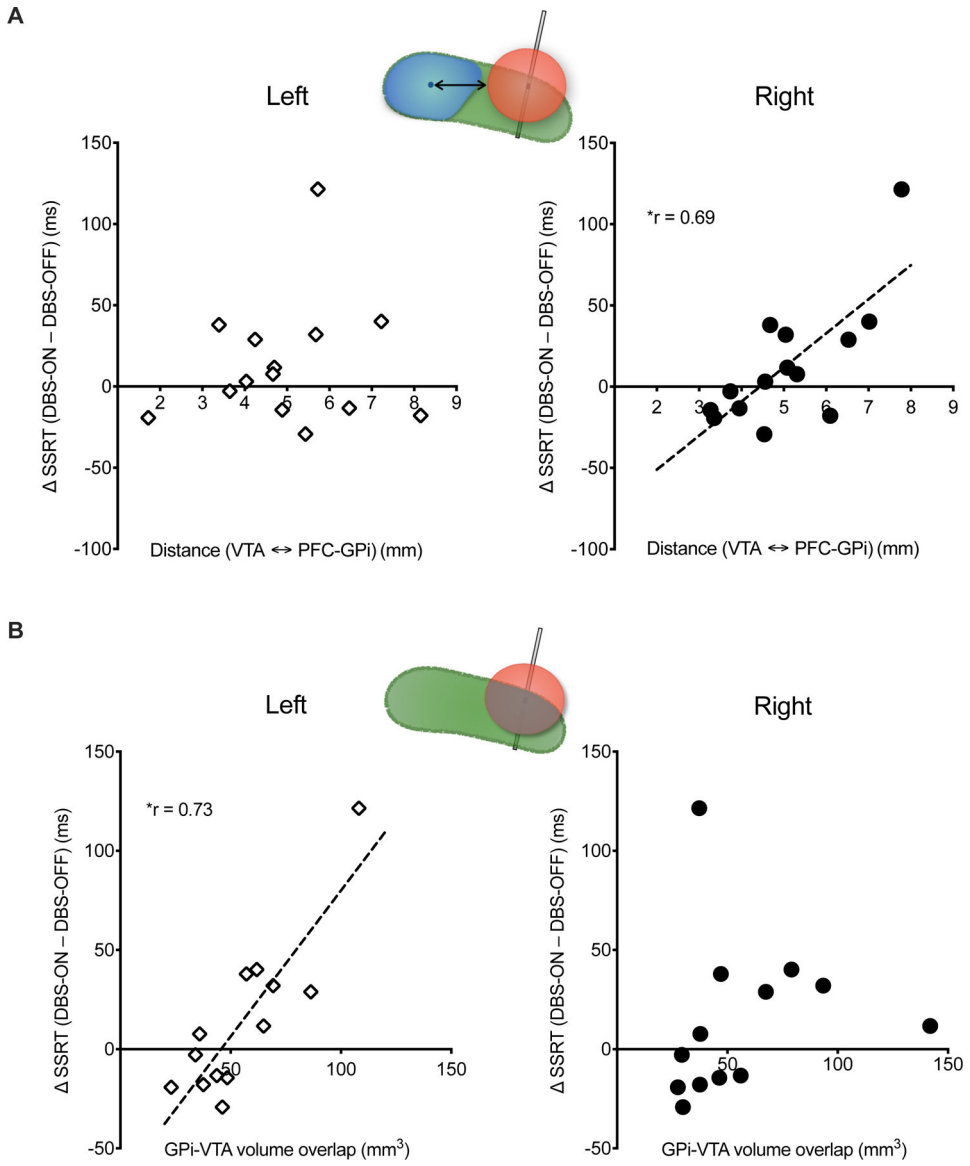

Figure 3. Stop-Signal Reaction Time and PFC-GPi Stimulation

Correlation between SSRT and DBS volume of tissue activation (VTA). (A) Shorter distance between the right PFC-GPi centroid and VTA is correlated with lower SSRT and reduced motor impulsivity. (B) Greater volumetric overlap between VTA and left GPi correlates with longer SSRT and increased impulsivity. Cartoons in each panel illustrate the metrics used in the correlation analysis (see Figure 1 C, D for details). Left and Right indicate left *vs.* right hemisphere DBS. r = Spearman's correlation coefficient. * indicates significance (p <0.05).

Table 1.

Demographic information of study participants

Characteristic	Patients (n = 7)
Age (Years)	62.7 ± 2.7
Disease Duration (Years)	13.0 ± 1.3
Duration of DBS Implantation (Months)	12.1 ± 1.5
MDS - UPDRS III Scale	32.6 ± 5.7
Handedness *	Right (5), Left (1)
Montreal Cognitive Assessment (MoCA) *	26.8 ± 1.1

MDS-UPDRS III Scale was obtained in the medication “on” state and with clinical DBS settings. Data are presented as mean ± S.E.M.

* Handedness and MoCA result of one study participant are unknown. Data are presented as mean ± S.E.M

Table 2.

Stop signal reaction time task performance

	DBS-OFF	DBS-ON ventral	DBS-ON dorsal	*p-value*
GO-RT (ms)	766 ± 26	728 ± 50	710 ± 51	0.57
Failed stop RT (ms)	569 ± 33	553 ± 40	591 ± 22	0.65
Overall SSD (ms)	325 ± 12	290 ± 25	295 ± 29	0.41
SSD after Convergence (ms)	380 ± 39	387 ± 38	430 ± 19	0.41
Response Accuracy (%)	79 ± 3	72 ± 6	73 ± 6	0.47
Go Discrimination Error (%)				
Go Omission Error (%)	15 ± 6	7 ± 1	10 ± 7	0.62
Probability of Stopping After Convergence (%)	46 ± 4	44 ± 4	44 ± 3	0.91
SSRT (ms)	335 ± 14	348 ± 26	323 ± 19	0.69

Go-RT = mean correct go reaction time; Failed stop RT = mean RT on failed stop trials; Overall SSD = mean stop signal delay in all stop trials; SSD after convergence = mean stop signal delay in stop trials after convergence; Response accuracy = % correct trials (stop and go trials); Go omission error = % omission error on go trials; probability of stopping after convergence = probability of stopping on stop trials after convergence; SSRT = mean stop signal reaction time (Go-RT – SSD after convergence), calculated for each subject then averaged. Data are presented as mean ± S.E.M.

Table 3.

Stimulation Settings of Participants

Participant Number	Lead Model	DBS-Ventral				DBS-Dorsal			
		Right		Left		Right		Left	
		Active Contact	Amplitude	Active Contact	Amplitude	Active Contact	Amplitude	Active Contact	Amplitude
1	Medtronic 3387™	C+, 8−	2 V	C+, 0−	2 V	C+, 9−	2 V	C+, 1−	2 V
2	Medtronic 3387™	C+, 8−	1.5 V	C+, 0−	1.5 V	9+, 10−	1.8 V	1+, 2−	1.8 V
3	Medtronic 3387™	C+, 9−	1 V	C+, 1−	2 V	C+, 10−	2 V	C+, 2−	2 V
4	Abbott St Jude 6173 ™	C+, 8−	3 mA	C+, 0−	3 mA	C+, 11A−, 11B−, 11C−	3 mA	C+, 3A−, 3B−, 3C−	2.5 mA
5	Abbott St Jude 6173 ™	C+, 11A−	3 mA	1+, 2B−	3.5 mA	C+, 12−	3.5 mA	C+, 3B−	3.5 mA
6	Abbott St Jude 6173 ™	C+, 10A−	3 mA	C+, 2B−	3 mA	C+, 11B−	3 mA	C+, 3B−	3 mA
7	Abbott St Jude 6173 ™	C+, 11A−	3 mA	1+, 2B−	3.5 mA	C+, 12−	3.5 mA	C+, 3B−	3.5 mA

Stimulation Settings of participants. Stimulation amplitudes of Medtronic Model 3387 and St Jude / Abbott Model 6173 were in units of Voltage (V) and milliamperes (mA), respectively. All participants had the leads with the same model implanted bilaterally.